Sustainability **2015**, *7*, 2066-2085; doi:10.3390/su7022066

OPEN ACCESS

sustainability

ISSN 2071-1050

www.mdpi.com/journal/sustainability

Article

Measurement and Numerical Simulation of Air Velocity in a Tunnel-Ventilated Broiler House

Eliseo Bustamante [1,2,†,*], Fernando-Juan García-Diego [3,†], Salvador Calvet [1,†], Antonio G. Torres [1,†] and Antonio Hospitaler [2,†]

[1] Institute of Animal Science and Technology, Universitat Politècnica de València, Camino de Vera s/n, 46022 Valencia, Spain; E-Mails: salcalsa@upvnet.upv.es (S.C.); atorres@dca.upv.es (A.G.T.)

[2] Department of Construction Engineering and Civil Projects, Universitat Politècnica de València, Camino de Vera s/n, 46022 Valencia, Spain; E-Mail: ahospitaler@cst.upv.es

[3] Department of Applied Physics (U.D. Industrial Engineering), Universitat Politècnica de València, Camino de Vera s/n, 46022 Valencia, Spain; E-Mail: fjgarcid@upvnet.upv.es

† These authors contributed equally to this work.

* Author to whom correspondence should be addressed; E-Mail: elbusgar@doctor.upv.es; Tel.: +34-96-387-9431; Fax: +34-96-387-7439.

Academic Editor: Marc A. Rosen

Received: 23 October 2014 / Accepted: 6 February 2015 / Published: 13 February 2015

Abstract: A building needs to be designed for the whole period of its useful life according to its requirements. However, future climate predictions involve some uncertainty. Thus, several sustainable strategies of adaptation need to be incorporated after the initial design. In this sense, tunnel ventilation in broiler houses provides high air velocity values (2–3 $m \cdot s^{-1}$) at animal level to diminish their thermal stress and associated mortality. This ventilation system was experimentally incorporated into a Mediterranean climate. The aim was to resolve these thermal problems in hot seasons, as (traditional) cross-mechanical ventilation does not provide enough air velocity values. Surprisingly, very little information on tunnel ventilation systems is available, especially in terms of air velocity. Using Computational Fluid Dynamics (CFD) and a multi-sensor system, the average results are similar (at animal level: 1.59 ± 0.68 $m \cdot s^{-1}$ for CFD and 1.55 ± 0.66 $m \cdot s^{-1}$ for measurements). The ANOVA for validation concluded that the use of CFD or measurements is not significant (p-value = 0.1155). Nevertheless, some problems with air velocity distribution were found and need to be solved. To this end, CFD techniques can help by means of virtual designs and scenarios providing information for the whole indoor space.

Keywords: sustainable design; adaptation and retrofit (A & R); broiler house; Mediterranean climate; tunnel ventilation; sensors; CFD

1. Introduction

A building needs to be designed according to its requirements for the entire period of its useful life. Among these requisites, the geographical location and the climatic situation are prominent design features. Thus, the indoor environments of broiler house building are strongly conditioned by the climatology. Unfortunately, the uncertainty arising from climate change and global warming also causes uncertainty in the building design and the facilities installed [1,2]. For these reasons, farms in areas of climatic uncertainty (e.g., Mediterranean climate) need to adapt their designs by means of sustainable strategies. To this end, new models of ventilation systems were incorporated after the initial conception of the building-farm design. Obviously, these experimental design adaptations and experimental ventilation systems must be analysed using scientific procedures (CFD techniques and direct measurements).

Nowadays, broiler rearing involves the use of highly developed technology. In fact, modern broiler buildings can be considered intelligent buildings in the fullest sense [3]. In these buildings, forced ventilation is the most commonly-used ventilation system [4–7], mainly through negative pressure-systems [6,7]. Mechanical ventilation allows higher density of the broilers than natural ventilation. Moreover, mechanicalventilation diminishes the thermal stress and mortality of the birds in summer seasons or extreme climate, as it improves the control and values of the ventilation rates. Recently, [8] affirmed that housing conditions had more impact than flock density on animal welfare. Despite the technical complexity of broiler buildings, discrete and repetitive episodes of high mortality occur every year in summer [9,10]. In the Mediterranean climate, these fatal episodes of thermal stress and broiler mortality have been accentuated under the effects of global warming and climate change. In this climate, cross-mechanical ventilation is the most widespread ventilation system in broiler production [11].

There are some important studies on the influence of excessively hot climate on broilers. [12] describes its influence on high mortality rates, a decrease in meat quality and reduced welfare; [13] refers to the losses in feed intake (−16.4%), losses in body weight (−32.6%) and higher feed conversation ratio (25.6%) when a broiler reaches an age of 42 days. [14] refers to the changes in the metabolism of the broilers and the need for thermoregulation to reduce the internal heat of the animals. In this thermoregulation, high air velocity values (~2 $m \cdot s^{-1}$) can help by increasing the convective flux heat of broilers and therefore decrease their thermal stress and associated mortality. [14] reports the effects on welfare of these high air velocities over the birds: they remove the hot air around the birds, adding to conventional heat loss, and they remove humid air from around the broiler's head, making panting more efficient and imparting a sense of wind chill. To meet these high air velocity needs, tunnel ventilation has been experimentally incorporated in some Mediterranean climate areas. Moreover, it is also crucial to relate the number of fans in action with the associated air velocity values at broiler level. This is essential to determine the optimal programming of the fans and/or inlet automatisms of these tunnel broiler buildings.

Mediterranean climate refers to the weather typical of the Mediterranean area (Spain, France, Italy, *etc.*), although it is also found in other geographic areas worldwide: sections of Central Asia, Western and South Australia, South Africa, central Chile, California (USA), *etc.* France is considered a reference in broiler building ventilation technology and exports its building and ventilation system models. Other nearby countries with this climate (e.g., Spain, Italy, Portugal, Greece...) adopted these models and ventilation. However, cross-mechanical ventilation is only an acceptable system for the moderate variant of this climate [6,7]. Nowadays, new ventilation systems (mechanical single sided, tunnel variants, *etc.*) are tested in areas (e.g., Spain) where cross-mechanical ventilation entails thermal problems. A feature of these adapted buildings is that air inlets are located in the lateral walls near the opposite façade to the fans, because in the original cross-mechanical ventilation systems the tendency was to build an office or control room there, which would remain in place when tunnel ventilation was installed.

In this work, we study a typical tunnel broiler building in Spain, using CFD techniques and a multi-sensor system [6] to determine the exact indoor environment of this imported ventilation system. To this end, CFD can be a powerful tool to analyse indoor environments of broiler houses and obtain the CFD results for the entire indoor space, whereas direct measurements only provide results for a limited number of points (the physical sensors). This analysis will serve to assess optimal management of the whole broiler building and, especially, the programming of the fans and inlets.

Earlier works have broadly used CFD techniques to study the internal microclimate of livestock buildings [15–18] and poultry buildings with other ventilation systems [7,11,19,20] and with tunnel ventilation under negative pressure-systems in [21–23]. Tunnel ventilation from broiler buildings is found in different countries, such as Brazil [21,22], Korea [23], USA [24] and countries with a tropical climate [25]. According to these references, tunnel ventilation achieves high air velocity values. On the other hand, in some of these designs, the fans are placed on the opposite façade to the inlets [25]. Nevertheless, in this article we study a variant of tunnel ventilation with the inlets at the lateral end [25] because in the original building design (with cross-mechanical ventilation) the control room precluded any other disposition.

To summarise: (i) we studied a typical tunnel broiler building in Spain; (ii) tunnel ventilation can be easily installed in all broiler buildings with only a retrofit of one wall to install the fans there; (iii) the study is carried out using CFD techniques and a multi-sensor system; (iv) the numerical results of air velocity are validated; (v) tunnel ventilation achieves high air velocity values to improve the birds' welfare in hot seasons; (vi) future optimisation of design and assessments is required to improve this ventilation system; and (vi) CFD techniques can help by providing virtual designs and scenarios using information from the whole indoor space.

2. Materials and Methods

2.1. The Building

A broiler building equipped with tunnel ventilation located at Alcalá de Xivert (Castellón-Spain) was studied. The upper left corner of Figure 1 shows the exterior façade, with the eight frontal exhaust fans and one lateral fan. In other corners are the interior of the building in three operations; the fans in operation were in white, to allow the sunlight to enter; and in the central image of Figure 1 is the multi-sensor system with sensors at two heights (0.25 m and 1.75 m).

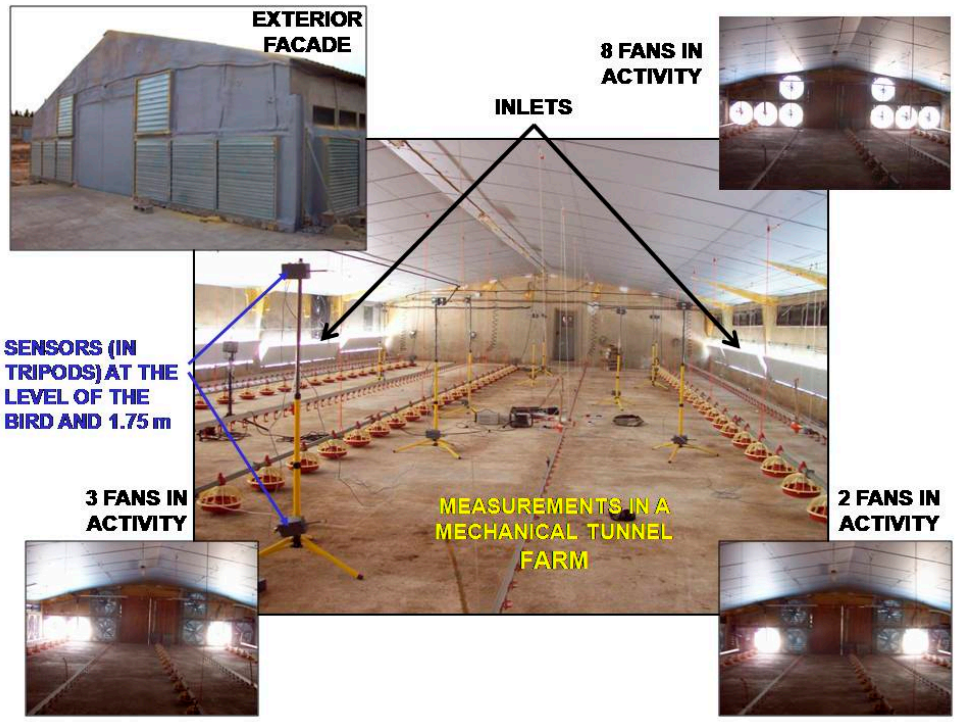

Figure 1. Measurements in the tunnel broiler building.

Building dimensions were: length, 120 m; width, 12.2 m; sidewall height 2.2 m; double pitched roof (slope 21.3%). The ventilation was equipped with ten exhaust fans (Model Euromunters EM 50n) with a diameter of 1.28 m, 1.1 kW of power consumption and nominal ventilation flow 42,125 m^3 h^{-1} at $\Delta P = 0$ Pa. Eight exhaust fans were located on the south façade (main façade) and the other two exhaust fans in the lateral façade, one fan in each lateral wall, near those located at the south façade as shown in Figure 1. The building was also equipped with twelve inlets measuring 4.7 × 0.45 m, placed at a height of 0.3 m, controlled by an automatic system of two groups of six inlets located in the lateral walls; all inlets were located near the north façade. The inlets are placed on the side walls because the control room is located behind the wall opposite the fans, preventing the fans being positioned there. According to Daghir [25], this is a variant of tunnel ventilation where the air entrance is equilibrated. The building was empty during the field experiments (as in other similar studies: [6,7,11,18,26]) to prevent the broilers undergoing sudden changes of pressure and air flow during the experiment.

This broiler building was built in 1983, and until a few years ago had natural ventilation, after which it was equipped with cross-mechanical ventilation; currently, it also has tunnel ventilation installed. The main orientations of walls and roofs were determined using a compass (we designated them North-Wall, South-Wall, East-Wall, West-Wall, East-Cover, West-Cover and floor, according to the main orientation reached).

2.2. Experimental Scenarios (Operations)

In this paper, the field experiments comprised nine experimental scenarios (operations) at different boundary conditions (BCs). By means of differential pressure sensors [6], differential pressure was fixed at a constant30 Pa—which, according to the farmer, was a typical differential pressure in the management of this building—and the number of fans running was gradually increased. First, two fans were activated,

and gradually we added one fan at a time until all eight fans on the south façade were on. Finally, the two lateral wall fans were also in action. (Operation I corresponds to two fans in action, Operation II with three fans in action, *etc.*, until Operation IX, with ten fans in action). Operation I began with two fans because no typical real operation in the building uses a single working fan. In the cooler winter months, high air velocity values are not required; then, a minimum number of fans working (2, 3 or 4 fans located near the floor) is enough. In hot seasons, the air velocity requirements are higher and it is necessary to activate more fans (the 5 or 6 fans located near floor level), triggering the rest of the fans (the two higher fans and the two laterals) if the weather is very hot. The two higher fans can improve the efficiency of the refrigeration system if it is activated (to improve indoor movement of the air on the whole).

To maintain the differential pressure at 30 Pa during these operations, the flaps of the inlets change by means of the automatic system.

2.3. CFD Background and Turbulence Models

CFD FLUENT (Fluent Inc., Lebanon, NH, USA) [27] was used to carry out the CFD simulations in this article. CFD FLUENT [27] had been used with great success in previous CFD simulations of poultry buildings, as mentioned previously [7,11,19,20,23].

CFD techniques solve a set of partial differential equations (PDEs) [15,28]: equations of continuity (Equation (1)), conservation of momentum (Navier-Stokes law) (Equation (2)) and the energy equation (Equation (3)).

$$\frac{\partial \rho}{\partial t} + \nabla(\rho \vec{v}) = S_m \tag{1}$$

$$\frac{\partial}{\partial t}(\rho\vec{v}) + \nabla(\rho\vec{v}\vec{v}) = -\nabla p + \nabla(\bar{\tau}) + \rho\vec{g} + \vec{F} \tag{2}$$

$$\frac{\partial}{\partial t}(\rho E) + \nabla(\vec{v}(\rho E + p)) = \nabla\left(k_{eff}\nabla T - \sum_j h_j \vec{J}_j + (\bar{\bar{\tau}}\vec{v}) \right) + S_h \tag{3}$$

Where ρ: fluid density (kg·m^{-3}); t: time (s); u, v, w: velocity (m·s^{-1}); S_m: mass source (kg·m^{-3}); p: pressure (Pa); τ: stress tensor (Pa); g: gravitational acceleration (m·s^{-2}); F: external force vector (N·m^{-3}); E: total energy (J); k_{eff}: heat transmission coefficient; T: temperature (K); h: specific enthalpy (J·kg^{-1}); S_h: total entropy (J·K^{-1}).

Reynolds-averaged Navier-Stokes equation (RANS) turbulence models are commonly used in the study of indoor environments of livestock buildings. Moreover, from the RANS turbulence models, the RNG k-ε model was chosen to carry out the CFD simulations. The standard k-ε turbulence model has been used by some authors [7,11] because it offers reasonable precision and easy convergence [29]. However, in this article, the RNG k-ε model (a variant of the standard k-ε turbulence) was used because it performs well. The RNG k-ε turbulence model includes additional terms for the dissipation rates, describing more the physical phenomenon in greater detail and improving the accuracy of the results. It should be noted that none of the existing turbulence models are complete, *i.e.*, their prediction performance is highly reliant on turbulent flow and geometry [15]. The transport equations of this turbulence model were 4 and 5 [27]:

$$\rho \frac{Dk}{Dt} = \frac{\partial}{\partial x_i}\left(\alpha_k \mu_{eff} \frac{\partial k}{\partial x_i} \right) + G_k + G_b - \rho\varepsilon - Y_M \quad (4)$$

$$\rho \frac{D\varepsilon}{Dt} = \frac{\partial}{\partial x_i}\left(\alpha_\varepsilon \mu_{eff} \frac{\partial k}{\partial x_i} \right) + C_{1\varepsilon} \frac{\varepsilon}{k}(G_k + C_{3\varepsilon} G_b) - C_{2\varepsilon}\rho \frac{\varepsilon^2}{K} - R \quad (5)$$

where k: turbulent kinetic energy ($m^2 \cdot s^{-2}$); α_k: the generation of kinetic energy due to the mean velocity gradient ($kg \cdot m^{-1} \cdot s^{-2}$); μ_{eff}: effective viscosity ($m^2 \cdot s$); G_k: the generation of kinetic energy due to the variations of the components of the average velocity of the flow ($kg \cdot m^{-1} \cdot s^{-2}$); G_b: the generation of kinetic energy by boundary push ($kg \cdot m^{-1} \cdot s^{-2}$); ε: turbulent dissipation rate ($m^2 \cdot s^{-3}$); α_ε: the generation of kinetic energy due to buoyancy ($kg \cdot m^{-1} \cdot s^{-2}$); Y_M: contribution of the pulsatile expansion associated to the compressible turbulence ($kg \cdot m^{-1} \cdot s^{-2}$); R: the gas-law constant ($8.314 \cdot 10^3$ $J \cdot kg \cdot mol^{-1} \cdot K^{-1}$); $C_{1\varepsilon}$: constant; $C_{2\varepsilon}$: constant; $C_{3\varepsilon} = \tanh[u_1/u_2]$; u_1: velocity of flow parallel to g_i (gravitational vector); u_2: velocity of flow perpendicular to g_i. Moreover, the constant values were $C_{1\varepsilon} = 1.42$, $C_{2\varepsilon} = 1.68$ [27,29].

In this article, we carried out nine three-dimensional CFD simulations, corresponding to nine tested scenarios (nine typical conditions of operation of the building).

2.4. Geometry, Mesh and BC

The geometry and mesh of the broiler building were performed in the pre-processor GAMBIT [30] (Geometry and Mesh Building Intelligent Toolkit) of FLUENT [27]. This building geometry was modelled in its real dimensions. The exhaust fans were modelled as circles 1.28 m in diameter and the twelve inlets were accurately modelled in the form adopted in each scenario as in similar studies [7,11,31].

Each scenario was mainly characterised by the number of fans operating, maintaining the differential pressure at 30 Pa [6]. In these setups, the ventilation rate was measured using the procedures of [32], although the fans are new and the values are very similar to those from the manufacturer. This measurement protocol [32] consisted of ducting the exhaust air 50 cm from the fan and then measuring by means of a hot wire anemometer at 24 different locations in the section, as indicated [33].

A mesh dependency test was performed, analysing four different meshes: Mesh 1 (516,055 cells & 105,427 nodes), Mesh 2 (908,025 cells & 174,979 nodes), Mesh 3 (1,937,181 cells & 363,604 nodes) and Mesh 4 (3,627,052 cells & 661,559 nodes). In this study, the numerical results are stabilised and minor differences are observed from Mesh 3 to Mesh 4. According to this mesh study, Mesh 4 was chosen. By this procedure, we ensure that the numerical results obtained are not affected by the grid.

The meshing comprised unstructured tetra and prism layers. Applying thin prism layers to the first rows near the surfaces provides a more accurate result near the boundary layers. In this way, the quality of the mesh is also studied using the equiangular skewness command in GAMBIT [30].

The geometry and mesh domain built in GAMBIT [30] was exported to the CFD-solver FLUENT [27]. Moreover, it was considered that the flow (air) is steady, three-dimensional, viscous, turbulent, incompressible and isothermal. The air properties are considered constants. Table 1 shows the properties of the air and associated values.

To link the pressure and the velocity, the SIMPLE algorithm was used [27] as well as the second order upwind scheme [28].

Table 1. Main inputs and BCs at CFD simulations.

CFD Simulation	Fans in Action	Total Mass Flux Rate (1) ($kg \cdot s^{-1}$)	Average of Air Velocity at Inlets ($m \cdot s^{-1}$)
I	2	24.68	0.83
II	3	37.02	1.23
III	4	49.36	1.61
IV	5	37.02	2.04
V	6	61.70	2.45
VI	7	74.04	2.85
VII	8	86.38	3.25
VIII	9	98.72	3.67
IX	10	111.06	4.04

(1) Measured by the procedures of [32].

The air velocity at inlets (windows) and mass flux rate of each outlet (fans) were BC used to carry out the CFD simulations. For each operation and considering negligible fluctuations of values, we assumed that the air velocity at all inlets was the same and the mass flux rate was the same for the fans, as in earlier studies [7,11]. The input of the air velocity at inlets was obtained from the measurements at each inlet using a Testo 425 hot-wire anemometer [34] (calibrated in a wind tunnel by Testo AG Lenzkirch (Spain) [34] according to UNE EN ISO 9001:2001), and the average from all inlets is the required input. The input of the ventilation rate of each fan was obtained using the protocol of [32]. Table 1 indicates the main computational settings and the cited BC.

Considering that the building was empty during the field experiments, the broiler presence was not modelled, nor other elements such as feeding and water equipment [7,11]. Obviously, CFD points with special relevance are the physical location points of the sensors. Figure 2a shows the grid in an inlet and Figure 2b the inlets in the building. In this Figure 2, we can observe that the inlets and associated flaps form an angle. This angle changes (from 4° to 38°) in order to maintain the differential pressure constant throughout the nine operations (30 Pa, in our field experiment).

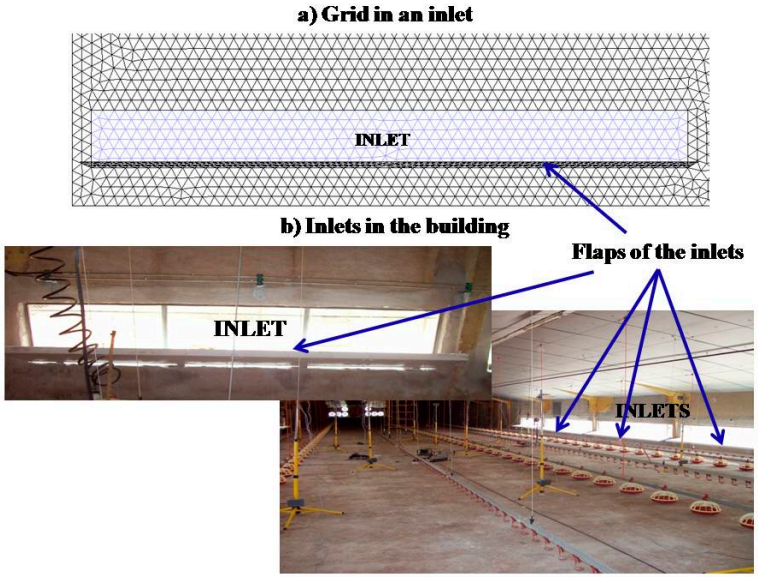

Figure 2. (**a**) Grid in an inlet; (**b**) Inlets in the building.

2.5. Validation of CFD Results

2.5.1. General Context: the Multi-Sensor System and Points of Measurement

The indoor turbulence intensity generated in mechanical ventilation of livestock buildings is very high (from 1% to 20%), with sudden changes in the air velocity values in the same coordinate throughout the experiment [6,7,35]. For this reason, a high-capacity measurement system is needed, both in number of sensors and number and quality of signals. The validation of CFD simulations [36] was thus carried out by means of a specific measuring system [6]. This measuring system consisted of air velocity sensors and differential pressure sensors and was able to acquire up to a maximum of 128 signals simultaneously at 5 s intervals. The sensors of air velocity were platinum resistance temperature detectors (RTD), the thin film detector was the Pt100 from Omega Inc. [37] and the differential pressure sensors were HCXM010D6Vs from Sensortechnics Inc. [38]. This measuring system is described in depth in [6]. In our case, only 32 sensors were read: 30 air velocity sensors and 2 differential pressure sensors [6]. The sensors were placed on 15 tripods at two heights: at adult broiler level 0.25 and at 1.75 m. These measurements were taken in three sections of the building: one section near the inlets, another section in a central zone (when the inlets were finished) and finally another section closer to the fans. The spatial distribution of the tripods was random, in an attempt to measure all areas of the test sections (central section, near the fans and the inlets). Moreover, Daghir [25] mentioned that the area of inlets and the area of fans are vital in the design of tunnel ventilation. At the centre of Figure 1, some tripods and the multi-sensor system in an operation are shown.

During this field experiment (10 min registering in each operation) we received the signals from the sensors. In each of the three sections for each operation we received 3600 measurements of air velocity (30 s × 10 min × 60/5 data/min); thus, a total of 97,200 air velocity measurements (3600 × 9 scenarios × 3 sections) were taken at the 9 scenarios and three sections. Figure 3 shows the test section and Table 2 the sensor coordinates.

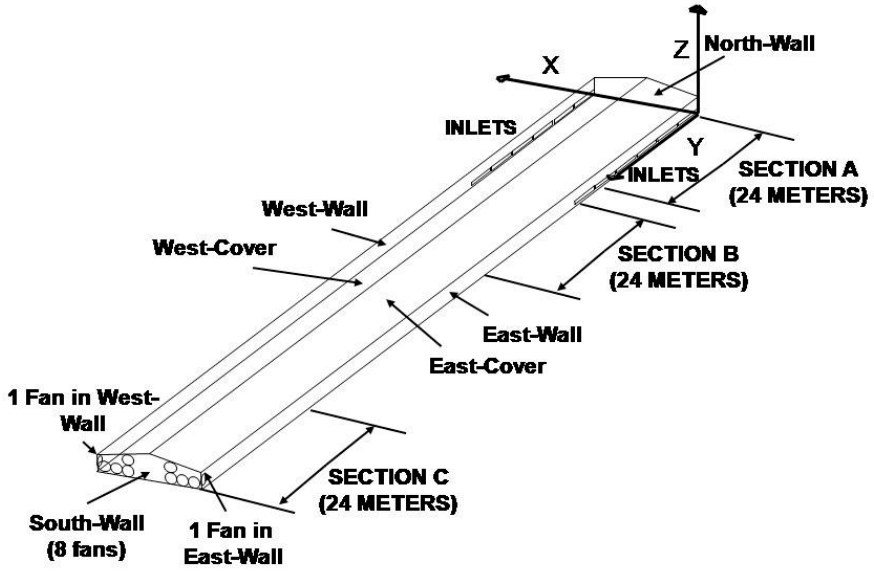

Figure 3. Test sections.

Table 2. Sensor coordinates.

Sensor number *	Section A		Section B		Section C	
	***X*-coordinate (*m*)**	***Y*-coordinate (*m*)**	***X*-coordinate (*m*)**	***Y*-coordinate (*m*)**	***X*-coordinate (*m*)**	***Y*-coordinate (*m*)**
1–2	5.56	4.34	5.92	32.14	5.87	99.23
3–4	5.39	8.42	5.62	36.54	5.42	103.90
5–6	5.83	13.64	5.73	43.25	5.69	108.76
7–8	5.61	16.51	8.57	39.36	5.58	110.33
9–10	10.66	22.78	9.47	43.32	9.89	118.02
11–12	8.16	18.65	10.60	40.22	8.78	115.14
13–14	7.18	19.17	9.00	39.36	10.03	116.25
15–16	5.50	20.20	9.04	36.88	6.21	118.93
17–18	2.22	3.87	1.50	29.20	1.86	96.48
19–20	2.52	7.06	3.47	33.65	2.94	101.15
21–22	3.45	11.24	3.92	39.21	3.75	107.40
23–24	10.61	3.55	11.48	34.83	11.26	98.06
25–26	8.74	9.86	5.83	48.17	9.13	105.18
27–28	1.54	19.54	1.54	52.00	2.34	117.49
29–30	2.81	15.76	0.82	47.00	3.11	113.07

***** The first sensors at animal level, the second at 1.75 m.

During the operations in the same section there was no change in the tripods' location, in order to measure and compare the fluctuations of values acquired as the number of fans in action increased. The 30 air velocity sensors (in their tripods) were moved from one section to another at each ventilation regime case.

2.5.2. Statistical Model and Variables

In the present article, the validation model consisted of a statistical procedure by means of an analysis of variance (ANOVA).

The validation model for this article is:

$$Y_{ijkl} = \mu + S_i + F_j + H_k + M_l + (S\times F)_{ij} + (S\times H)_{ik} + (S\times M)_{il} + (F\times H)_{jk} + (F\times M)_{jl} + (H\times M)_{kl} + (S\times F\times H)_{ijk} + (S\times F\times M)_{ijl} + (S\times H\times M)_{ikl} + (F\times H\times M)_{jkl} + (S\times F\times H\times M)_{ijkl} + \varepsilon_{ijkl} \quad (6)$$

where the different variables and interactions are explained below:

Y_{ijkl}: Air velocity in the section *i* with *j* Fans in action at Height *k* and by the methodology *l*;

S_i: Measurement section (3);

F_j: Fans in action (9);

H_k: Height of the sensor (2);

M_l: Methodology: CFD *vs.* direct measurements by multi-sensor system (2);

$(S\times F)_{ij}$: Interaction between Section-Fan (27);

$(S\times H)_{ik}$: Interaction between Section-Height (6);

$(S\times M)_{il}$: Interaction between Section-Methodology (6);

$(F\times H)_{jk}$: Interaction between Fans-Height (18);

$(F \times M)_{jl}$: Interaction between Fans-Methodology (18);
$(H \times M)_{kl}$: Interaction between Height-Methodology (4);
$(S \times F \times H)_{ijk}$: Triple interaction between Section-Fan-Height (54);
$(S \times F \times M)_{ijl}$: Triple interaction between Section-Fan-Methodology (54);
$(S \times H \times M)_{ikl}$: Triple interaction between Section-Height-Methodology (12);
$(F \times H \times M)_{jkl}$: Triple interaction between Fan-Height-Methodology (36);
$(S \times F \times H \times M)_{ijkl}$: Fourfold interaction between Section-Fan-Height-Methodology (108);
ε_{ijkl}: Error of the model.

Numbers in parentheses indicated number of factors. To study these effects, all factors were considered random. The model was analysed using the GLM procedure from SAS systems [39]. We shall perform an initial analysis to obtain first results. The non-significant interactions will then be eliminated from the model, and another analysis will be conducted to obtain the refined results. Using this procedure, the model will have improved results, making the significant effects more robust.

2.5.3. Regression Line (CFD *vs.* Measurements)

To compare the CFD results and the measurements, a linear regression is proposed. The model of this linear regression is:

$$V_{CFD} = \alpha + \beta \times V_{meas} \tag{7}$$

where,

V_{meas} is the average of the measured air velocity values
V_{CFD} is the air velocity obtained in the CFD simulations

2.5.4. Relative Error at Each Point

The indoor turbulence in broiler buildings equipped with mechanical ventilation is high [6,7,35]. Thus, the fluctuations of the air velocity values at the same point over time may be relevant [6]. We used a robust measurement system in terms of number of sensors and in received signals; nevertheless, it is necessary to test a possible relative error in the *i* studied points. This relative error in the *i* point (E_i) can be defined as:

$$E_i = \frac{V_{meas} - V_{CFD}}{V_{meas}} \tag{8}$$

where:

V_{meas} is the average of the measured air velocity using the multi-sensor system at point *i* taken as the real air velocity, and
V_{CFD} is the air velocity obtained in the CFD simulations at point *i*.

3. Results

3.1. Results of the Validation Model

In Table 3, we can see the ANOVA results for the proposed validation model after the refinement. The main result is that the "Methodology" variable is not significant (p-value < 0.1155), nor are the interactions; *i.e.*, there is no difference between using the CFD techniques or the direct measurements using the multi-sensor system. At this point and by means of these results from Table 3, we validated the CFD results for air velocity.

Table 3. ANOVA of air velocity in different scenarios.

Variables	DF	Sum of Squares	Mean Square	F-ratio	*p*-value
Section	2	33.10	16.55	149.07	<0.0001
Fans	8	555.09	69.39	625.08	<0.0001
Height	1	1.07	1.07	9.61	0.0020
Methodology	1	0.28	0.28	2.48	0.1155
Section × Fan	16	45.75	2.86	25.76	<0.0001
Section × Height	2	21.18	10.59	95.42	<0.0001
Fans × Height	8	5.88	0.73	6.62	<0.0001
Error	1581	175.50	0.111		

According to the proposed linear regression for the 90 points studied (physical location of the sensors), we obtained a dependent term near one (+1.7%) and an independent term near zero (−0.1%). Moreover, we obtained a coefficient of determination of 0.98. In Figure 4, we can see this linear regression.

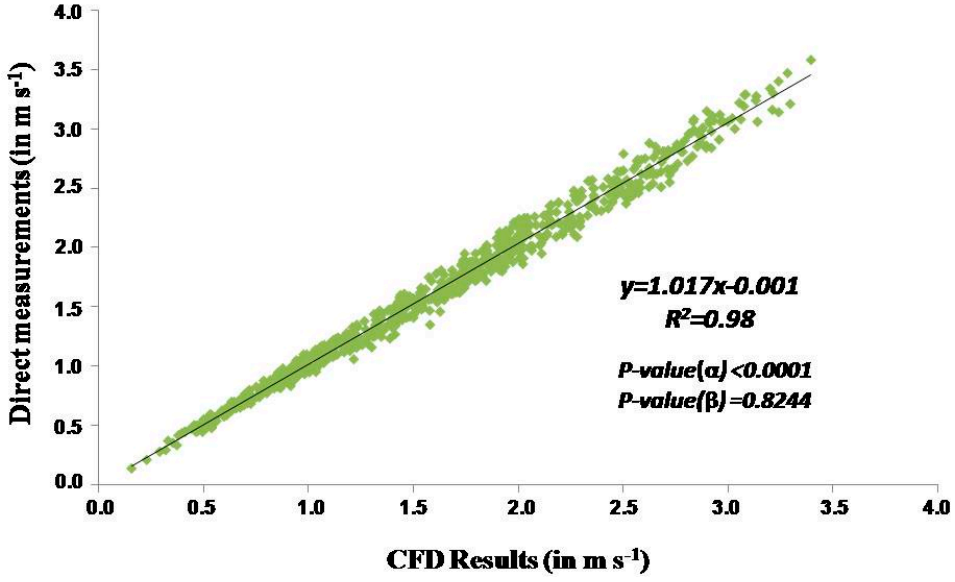

Figure 4. Regression curve of CFD results *vs.* direct measurements in the studied 90 points.

3.2. CFD Results and the Direct Measurements

CFD-air velocity results and the measurements using the multi-sensor system have similar values, as shown in Table 4.

Table 4. Air velocity in $m \cdot s^{-1}$ (average ± standard deviation) in the field experiment based on direct measurements and CFD simulations. The number of averaged data is indicated in parenthesis.

Operation	Height	Methodology	Section A	Section B	Section C	Average
I	0.25 m	Measured	0.75±0.24 (15)	0.66 ± 0.18 (15)	0.47 ± 0.11(15)	0.63 ± 0.22(45)
		CFD	0.77 ± 0.20(15)	0.69 ± 0.18(15)	0.49 ± 0.12(15)	0.65 ± 0.21(45)
	1.75 m	Measured	0.62 ± 0.22 (15)	0.56 ± 0.11(15)	0.58 ± 0.09(15)	0.59 ± 0.15(45)
		CFD	0.62 ± 0.22(15)	0.60 ± 0.12(15)	0.60 ± 0.10(15)	0.61 ± 0.15(45)
	Average	Measured	0.69 ± 0.24 (30)	0.61 ± 0.16(30)	0.53 ± 0.12 (30)	0.61 ± 0.19 (90)
		CFD	0.70 ± 0.22 (30)	0.64 ± 0.16 (30)	0.55 ± 0.13 (30)	0.63 ± 0.18 (90)
II	0.25 m	Measured	1.15 ± 0.35 (15)	1.01 ± 0.24 (15)	0.69 ± 0.14 (15)	0.95 ± 0.32 (45)
		CFD	1.16 ± 0.30 (15)	1.05 ± 0.25 (15)	0.71 ± 0.13 (15)	0.97 ± 0.30 (45)
	1.75	Measured	0.85 ± 0.27 (15)	0.84 ± 0.16 (15)	0.84 ± 0.16 (15)	0.84 ± 0.20 (45)
		CFD	0.90 ± 0.31 (15)	0.88 ± 0.18 (15)	0.90 ± 0.18 (15)	0.89 ± 0.23 (45)
	Average	Measured	1.00 ± 0.34 (30)	0.92 ± 0.22 (30)	0.76 ± 0.17 (30)	0.89 ± 0.27 (90)
		CFD	1.03 ± 0.33 (30)	0.97 ± 0.23 (30)	0.80 ± 0.18 (30)	0.93 ± 0.27 (90)
III	0.25 m	Measured	1.42 ± 0.41 (15)	1.28 ± 0.31 (15)	0.91 ± 0.24 (15)	1.20 ± 0.38 (45)
		CFD	1.43 ± 0.38 (15)	1.29 ± 0.26 (15)	0.95 ± 0.25 (15)	1.22 ± 0.36 (45)
	1.75 m	Measured	1.11 ± 0.36 (15)	1.13 ± 0.24 (15)	1.20 ± 0.22 (15)	1.15 ± 0.28 (45)
		CFD	1.13 ± 0.36 (15)	1.20 ± 0.28 (15)	1.22 ± 0.20 (15)	1.19 ± 0.29 (45)
	Average	Measured	1.26 ± 0.41(30)	1.21 ± 0.28 (30)	1.05 ± 0.27 (30)	1.17 ± 0.33 (90)
		CFD	1.28 ± 0.40(30)	1.24 ± 0.27 (30)	1.09 ± 0.26 (30)	1.20 ± 0.32 (90)
IV	0.25 m	Measured	1.50 ± 0.35 (15)	1.57 ± 0.34 (15)	1.15 ± 0.22 (15)	1.40 ± 0.36 (45)
		CFD	1.57 ± 0.36 (15)	1.64 ± 0.36 (15)	1.17 ± 0.22 (15)	1.46 ± 0.38 (45)
	1.75 m	Measured	1.28 ± 0.35 (15)	1.43 ± 0.24 (15)	1.46 ± 0.23 (15)	1.39 ± 0.28 (45)
		CFD	1.32 ± 0.40 (15)	1.47 ± 0.28 (15)	1.51 ± 0.22 (15)	1.43 ± 0.31 (45)
	Average	Measured	1.39 ± 0.36 (30)	1.50 ± 0.30 (30)	1.30 ± 0.27 (30)	1.40 ± 0.32 (90)
		CFD	1.44 ± 0.40 (30)	1.55 ± 0.33 (30)	1.34 ± 0.28 (30)	1.45 ± 0.34 (90)
V	0.25 m	Measured	1.61 ± 0.29 (15)	1.81 ± 0.31 (15)	1.39 ± 0.30 (15)	1.60 ± 0.35 (45)
		CFD	1.67 ± 0.34 (15)	1.89 ± 0.33 (15)	1.40 ± 0.32 (15)	1.66 ± 0.38 (45)
	1.75 m	Measured	1.38 ± 0.33 (15)	1.71 ± 0.27 (15)	1.76 ± 0.24 (15)	1.62 ± 0.33 (45)
		CFD	1.45 ± 0.38 (15)	1.75 ± 0.32 (15)	1.82 ± 0.23 (15)	1.67 ± 0.35 (45)
	Average	Measured	1.49 ± 0.33 (30)	1.76 ± 0.29 (30)	1.57 ± 0.33 (30)	1.61 ± 0.33 (90)
		CFD	1.56 ± 0.37 (30)	1.82 ± 0.33 (30)	1.61 ± 0.34 (30)	1.66 ± 0.36 (90)
VI	0.25 m	Measured	1.63 ± 0.33 (15)	2.12 ± 0.36 (15)	1.60 ± 0.31 (15)	1.78 ± 0.40 (45)
		CFD	1.69 ± 0.37 (15)	2.20 ± 0.35 (15)	1.62 ± 0.31 (15)	1.84 ± 0.43 (45)
	1.75 m	Measured	1.48 ± 0.34 (15)	2.03 ± 0.37 (15)	2.00 ± 0.29 (15)	1.84 ± 0.42 (45)
		CFD	1.56 ± 0.40 (15)	2.04 ± 0.35 (15)	2.09 ± 0.28 (15)	1.90 ± 0.42 (45)
	Average	Measured	1.55 ± 0.34 (30)	2.08 ± 0.36 (30)	1.80 ± 0.36 (30)	1.81 ± 0.41 (90)
		CFD	1.63 ± 0.39 (30)	2.12 ± 0.35 (30)	1.85 ± 0.38 (30)	1.87 ± 0.42 (90)
VII	0.25 m	Measured	1.77 ± 0.36 (15)	2.40 ± 0.34 (15)	1.83 ± 0.37 (15)	2.00 ± 0.45 (45)
		CFD	1.83 ± 0.36 (15)	2.52 ± 0.36 (15)	1.85 ± 0.40 (15)	2.06 ± 0.49 (45)
	1.75 m	Measured	1.61 ± 0.43 (15)	2.27 ± 0.36 (15)	2.33 ± 0.32 (15)	2.07 ± 0.49 (45)
		CFD	1.69 ± 0.49 (15)	2.35 ± 0.40 (15)	2.41 ± 0.30 (15)	2.15 ± 0.51 (45)
	Average	Measured	1.69 ± 0.40 (30)	2.33 ± 0.35 (30)	2.08 ± 0.42 (30)	2.03 ± 0.47 (90)
		CFD	1.76 ± 0.43 (30)	2.43 ± 0.39 (30)	2.13 ± 0.45 (30)	2.11 ± 0.50 (90)

Table 4.*Cont.*

Operation	Height	Methodology	Section A	Section B	Section C	Average
VIII	0.25 m	Measured	1.74 ± 0.45 (15)	2.58 ± 0.29 (15)	2.03 ± 0.42 (15)	2.12 ± 0.52 (45)
		CFD	1.77 ± 0.48 (15)	2.72 ± 0.31 (15)	2.07 ± 0.42 (15)	2.19 ± 0.56 (45)
	1.75 m	Measured	1.76 ± 0.55 (15)	2.63 ± 0.32 (15)	2.55 ± 0.35 (15)	2.32 ± 0.61 (45)
		CFD	1.85 ± 0.60 (15)	2.68 ± 0.34 (15)	2.69 ± 0.35 (15)	2.41 ± 0.59 (45)
	Average	Measured	1.75 ± 0.49 (30)	2.61 ± 0.30 (30)	2.30 ± 0.46 (30)	2.22 ± 0.55 (90)
		CFD	1.81 ± 0.53 (30)	2.71 ± 0.32 (30)	2.38 ± 0.49 (30)	2.30 ± 0.58 (90)
IX	0.25 m	Measured	1.79 ± 0.50 (15)	2.59 ± 0.44 (15)	2.35 ± 0.47 (15)	2.24 ± 0.57 (45)
		CFD	1.88 ± 0.54 (15)	2.68 ± 0.53 (15)	2.37 ± 0.49 (15)	2.31 ± 0.61 (45)
	1.75 m	Measured	1.91 ± 0.61 (15)	2.83 ± 0.26 (15)	2.75 ± 0.33 (15)	2.50 ± 0.59 (45)
		CFD	2.00 ± 0.66 (15)	2.97 ± 0.27 (15)	2.92 ± 0.37 (15)	2.63 ± 0.64 (45)
	Average	Measured	1.85 ± 0.55 (30)	2.71 ± 0.38 (30)	2.55 ± 0.45 (30)	2.37 ± 0.59 (90)
		CFD	1.94 ± 0.60 (30)	2.82 ± 0.44 (30)	2.65 ± 0.51 (30)	2.47 ± 0.64 (90)
All	0.25 m	Measured	1.48 ± 0.48 (135)	1.78 ± 0.73 (135)	1.38 ± 0.67 (135)	1.55 ± 0.66 (405)
		CFD	1.53 ± 0.50 (135)	1.85 ± 0.77 (135)	1.40 ± 0.67 (135)	1.59 ± 0.68 (405)
	1.75 m	Measured	1.33 ± 0.56 (135)	1.72 ± 0.79 (135)	1.72 ± 0.76 (135)	1.59 ± 0.73 (405)
		CFD	1.39 ± 0.60 (135)	1.77 ± 0.82 (135)	1.79 ± 0.80 (135)	1.65 ± 0.77 (405)
	Average	Measured	1.41 ± 0.53 (270)	1.75 ± 0.76 (270)	1.55 ± 0.74 (270)	1.57 ± 0.70 (810)
		CFD	1.46 ± 0.56 (270)	1.81 ± 0.80 (270)	1.60 ± 0.76 (270)	1.62 ± 0.73 (810)

Despite the fact that the CFD simulations are performed in steady state (obtaining a single value for a point), the number of averaged data leads to results in this form similar to those of the direct measurements (average ± standard deviation). The studied 90 points (30 points in each section, 15 points at 0.25 m and 15 points at 1.75 m) by the 9 scenarios leads to 810 data (810 data for CFD and 810 data for direct measurements). At broiler level (0.25 m), the average (an average of 405 data for CFD and 405 data for direct measurements) of the air velocity values is very similar in CFD (1.59 ± 0.68 $m \cdot s^{-1}$) and by means of the direct measurements (1.55 ± 0.66 $m \cdot s^{-1}$).

3.3. Results of the Relative Error at Each Point

Despite the fact that the average air velocity value is very similar when comparing CFD and direct measurements, as seen in Table 4, the relative error defined in Equation (8) at some points is occasionally significant. Figure 5 shows this relative error.

Figure 5 shows the discrepancies of the relative error. The red triangle indicates the maximum and minimum error in each section. In Section A, the maximum error was 12.7% (Operation I) and the minimum was −14.5% (Operation III); in Section B, the maximum error was 12.6% (Operation III) and the minimum was −6.9% (Operation VI) and in Section C, the maximum error was 12.1% (Operation I) and the minimum was −11.0% (Operation III). The results for these relative errors are common and in the expected ranges, as they do not exceed 20% [40]. Moreover, the averaged relative error is small and very similar in all sections (+1.7% in Section A, +2.07% in Section B and +1.25% in Section C).

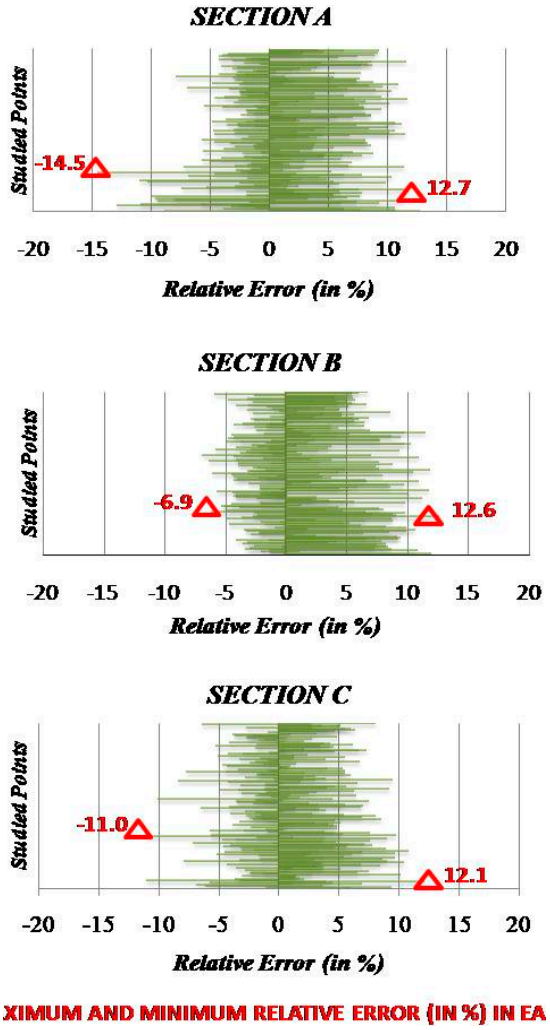

Figure 5. Relative error in each operation.

3.4. CFD-Air Velocity Results

CFD simulations provide very visual and interesting outputs that give an idea of the trends in air flow and an estimation of values by vectors or colours.

Figure 6 shows the air velocity values by colours at broiler level (0.25 m) in a typical operation (Operation IV, 5 fans in action) in summer seasons. Here, we can clearly observe three different indoor behaviours in terms of air velocity distribution. Near the inlets, we can see a zone with very heterogeneous values, where very high air velocity values are found close to an area with very low values ("dead zone"). In the central zone, we observe homogeneous air velocity values (very good area). Near the fans, we can again observe the heterogeneity of the air velocity values, notably the high air velocity values near the fans, which can seriously disturb the birds ("damaging zone"), causing feeding or health problems (colds, respiratory diseases) [41].

It is necessary to distinguish the use of this ventilation system for winter (cold seasons) or summer (hot seasons). As shown in Figure 6, all the air enters via Section A (inlets section); in summer, only air velocity is required, but in winter it is also necessary to heat the cold air. In cross-ventilation systems, the air inlets are located along the whole length of the building and less energy is needed to heat the incoming air than in a shorter entry section to the tunnel ventilation.

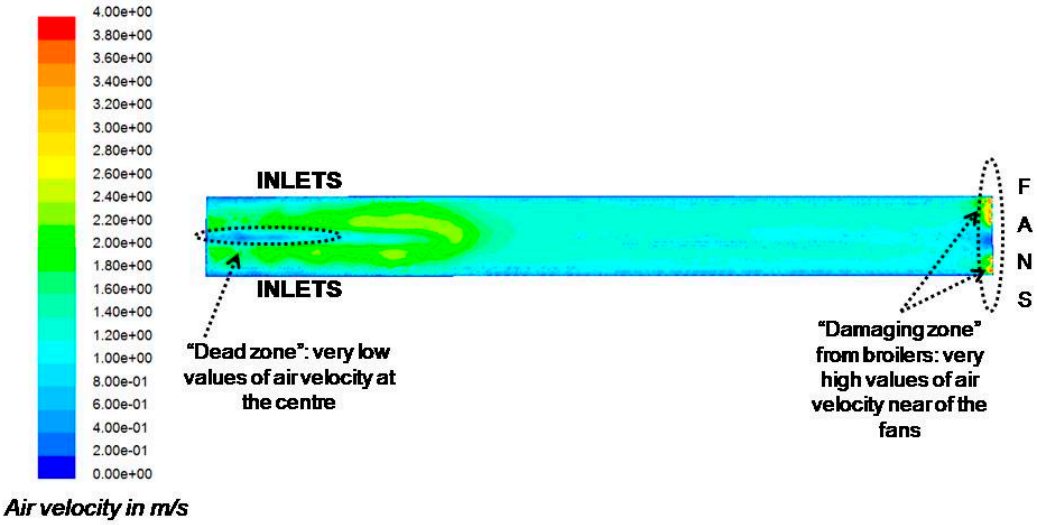

Figure 6. Air velocity values at broiler level (0.25 m) in the Operation IV.

4. Discussion

In this paper, we have analysed air velocity values in tunnel ventilation in a broiler building in Spain (Mediterranean climate). Whereas this ventilation system is quite commonplace in some countries [24,25], it has only recently been incorporated in countries with a medium-extreme Mediterranean climate. The aim of adopting this ventilation system is to resolve repetitive mortality and stress for the animals in summer, accentuated by the effects of climate change and global warming.

As this ventilation system has only recently been installed in these areas due to the widespread use of cross-mechanical ventilation, no published article addressing management and the air velocity distribution *vs.* fans in action could be found. This issue is crucial to optimise the management of these buildings. In this article, we respond to this question using powerful methodologies such as CFD and a multi-sensor system that also validated the numerical simulations. After the validation, CFD techniques can play an important role in developing virtual buildings and BCs in order to choose the best designs and managements. Moreover, they can provide information on the whole indoor environment, whereas the number of physical sensors is limited.

The field experiment took place in a broiler building in the Valencian Community (Spain), but it must be emphasised that there are diverse subclimatic areas within large countries such as Spain, and adopting a uniform ventilation system for the whole country is not an ideal solution.

In this article, we address the indoor air velocity distribution; obviously, other environmental parameters such as temperature or relative humidity are also relevant, especially if the broiler building is occupied. Along these lines, some interesting articles on occupied broiler buildings in other climatic areas were found, related to temperature [21] and the temperature and ammonia distribution [23]. Since we found that the air temperature had already been analysed by [21,23] and due to limitations on the length of this article, we focused only on the air velocity distribution as the crucial parameter for our needs and for automation of the broiler building.

Hence, an excessive number of fans working will waste unnecessary energy, cause colds in broilers or decrease the consumption of feed or water, whereas an insufficient number of fans running will lead to thermal stress and associated mortality.

The field experiments took place at a constant differential pressure measured as per[6], and the number of fans in action was gradually increased from two fans to ten fans in order to compare air velocity development, as indicated in Table 4. According to the specific literature on tunnel ventilation [25], the inlets area and fans area are key in tunnel ventilation design; thus, almost three main areas need to be analysed (near fans, near inlets and the intermediate area). Moreover, due to the large dimensions of the building and as indicated in the literature, the measurements only covered these areas of the building (Section A, Section B and C). As the building has no background of mortality in specific points and this ventilation system had recently been installed, the location of the tripods was randomly trying to cover the entire area of the study.

CFD simulations and direct measurements will confirm these three sections have different air velocity behaviour. In this sense, Figure 6 shows this different behaviour in terms of air velocity distribution:

(1). Section A showed great changes in air velocity and trajectories; we find a "dead zone" (very low air velocities) very close to zones with high values and turbulence.
(2). Section B was very homogeneous in air velocity distribution and presented high values if several fans were working; the trajectories did not show multi-directionality, as they are almost perpendicularly oriented to the fans.
(3). Section C showed very high air velocity values with a discrete number of fans working; air velocity trajectories are oriented to the fans the same as in Section B, but the air velocity values were higher than in Section B mainly when the number of fans was increased.

One simple assumption in tunnel ventilation is to calculate the air exchange and to divide it by the section [25]; the result is estimative, because it is assumed equal for the whole horizontal plane and this is not true, as shown in Figure 6. Turbulence, roughness or the assumptions of dimensions give rise to estimative results in comparison with accurate methods such as CFD or direct measurements. CFD also provides the trends of airflow in planes as we can see in Figure 6. For example, in the case of the Operation IV, the air exchange of the five fans is 190,000 $m^3 \cdot h^{-1}$(38,000 $m^3 \cdot h^{-1}$ × 5 fans), the section is 34.77 m^2; thus, 190,000/34.77 = 5464.48 $m \cdot h^{-1}$(=1.52 $m \cdot s^{-1}$) while the CFD results are 1.45 ± 0.34 $m \cdot s^{-1}$(Table 4) and for direct measurements the outcomes are 1.40 ± 0.30 $m \cdot s^{-1}$. The results are similar in finding discrepancies in this method for the above mentioned reasons (turbulence, roughness...).

In Table 4, we can see very high air velocity values if the number of fans working is increased; these values can be dangerous for the broilers, as they may suffer from colds, respiratory diseases or feeding problems.

According to Table 4 and Figure 6, tunnel ventilation is a good system to lower heat in broilers and the associated mortality, as it achieves high air velocity values. At broiler level, the maximum air velocity was 2.72 ± 0.31 $m \cdot s^{-1}$ (CFD) and 2.58 ± 0.29 $m \cdot s^{-1}$ (measured) in Operation VIII, Section B and the minimum was 0.49 ± 0.12 $m \cdot s^{-1}$ (CFD) and 0.47 ± 0.11 $m \cdot s^{-1}$(measured) in Operation I, Section C.

The Validation model for CFD simulations concluded that the variable "Methodology" (results by CFD simulations or direct measurements) and its interactions were not significant, as shown in Table 3. So, there is no difference between the use of these direct measurements or the corresponding CFD simulations to explore indoor air velocity in a tunnel ventilated broiler building, as in other similar studies of other ventilation systems [7]. Therefore, CFD procedures are confirmed as suitable to explore this ventilation system using virtual geometries. Although we can obtain the exact values of air velocities using CFD

simulations, as shown in Table 4, with CFD simulations we can also obtain excellent visual displays that provide a lot of information on the air flow characteristics and magnitude, as in Figure 6. After the good compromise between measurements and CFD, the main reason to have a dead zone is the location of the inlets in the lateral walls. If the tunnel building had the inlets in the opposite wall to the fans, this "dead zone" would disappear, according to some virtual CFD simulations to be developed in future works. Of course, tunnel ventilation has a predominant dimension in air velocity (the longitudinal axis) and we observed minor deviations between measurements and CFD results. These small deviations are found in all sections, with the least punctual (maximum and minimum) relative error in the central section (Figure 5), as it is the most one-dimensional. However, the averaged relative error is very similar and small in all the sections. The amount of the data minimises the deviations in the averaged relative error. The sources of these errors can come from both sides (the CFD or the direct measurements).

A broiler building which installs both mechanical ventilation systems (cross and tunnel) can be an interesting design. Combined periods using each ventilation system can be developed (cross in cold periods and tunnel in warm periods). In any case and in terms of air velocity values (obtained in Table 4), tunnel ventilation can be used for cold and warm periods.

In subsequent studies, it will be interesting to compare empty and occupied broiler buildings by the specific nature of the broiler metabolism. In any case, an empty building is a permanent state to be analysed in depth. In fact, in this building, the level of occupation can be 22,000 broilers. A one-day-old broiler weighs around 44 grams and a broiler on the last day of rearing has a weight of 4202 grams [42]. The broiler metabolism at different levels and the same type of birds (also the feather, *etc.*) will lead to great changes in the measurements and numerical results. In this sense, it will be necessary to adapt the measurement system for the tough conditions in occupied broiler buildings.

5. Conclusions

In this study, a CFD model of tunnel ventilated broiler building has been validated with direct measurements. No statistical difference has been found between measured and modelled data and therefore this model allows exploring practical management options of a tunnel ventilated building.

Under warm conditions, tunnel ventilation is adequate in general terms to achieve a proper air velocity for broilers with a relatively low number of fans in action. CFD simulations allow prediction of the behaviour of airflow under different circumstances. This is essential information to optimise the management of tunnel ventilation.

A tunnel ventilation system with lateral air entrances at one end of the building and exhaust fans at the other end, and three areas were identified according to ventilation patterns. Most of the building area achieves an adequate air velocity distribution for broiler growth under warm conditions. However, ventilation patterns are not optimal near building ends due to dead areas or excessive air velocity. Therefore, design of tunnel ventilation systems could be improved to avoid or minimise this effect and contribute to a sustainable broiler production.

Acknowledgments

This work was funded by the project GV04B-511 (Generalitat Valenciana, Spain) and by the Vicerrectorado of Investigación of the Universitat Politècnica de València (Programa de Apoyo a la Investigación y Desarrollo Multidisciplinar Project PAID register 2614).

Author Contributions

All the authors read and approved the final manuscript. All the authors contributed equally in this manuscript. Antonio Hospitaler is the general supervisor of the manuscript and wrote the introduction, Antonio G. Torres developed the statistics and wrote this part (Sections 2.5, 3.1 and 3.3), Salvador Calvet performed the field experiments, wrote the conclusions and revised the English of the whole manuscript, Fernando J. García-Diego revised the sensors and also performed the field experiments writing Sections 2.1, 2.2 and 2.5.1 and Eliseo Bustamante performed the CFD simulations and wrote the rest of the manuscript (Abstract, Sections 2.3, 2.4, 3.2, 3.4 and the Discussion).

Conflicts of Interest

The authors declare no conflict of interest.

References

1. Holmes, M.J.; Hacker, J.N. Climate change, thermal comfort and energy: Meeting the design challenges of the 21st century. *Energ. Build.* **2007**, *39*, 802–814.
2. Nardone, A.; Ronchi, B.; Lacetera, N.; Ranieri, M.S.; Bernabucci, U. Effects of climate changes on animal production and sustainability of livestock systems. *Livest. Sci.* **2010**, *130*, 57–69.
3. Clements-Croome, T.D.J. What do we mean by intelligent buildings? *Automat. Constr.* **1997**, *6*, 395–400.
4. Charles, D.; Walker, A. *Poultry Environment Problems: A Guide to Solutions*, 1st ed.; Charles, D., Walker, A., Eds.; Nottingham University Press: Nottingham, UK, 2002.
5. MWPS (Midwest Plan Service). *Mechanical Ventilating Systems for Livestock Housing*, 1st ed.; Midwest Plan Service, Iowa State University: Ames, IA, USA, 1990.
6. Bustamante, E.; Guijarro, E.; García-Diego, F.J.; Balasch, S.; Torres, A.G. Multisensor system for isotemporal measurements to assess indoor climatic conditions in poultry farms. *Sensors* **2012**, *12*, 5752–5774.
7. Bustamante, E.; García-Diego, F.J.; Calvet, S.; Estellés, F.; Torres, A.G. Exploring Ventilation Efficiency in Poultry Buildings: The Validation of Computational Fluid Dynamics (CFD) in a Cross-Mechanically Ventilated Broiler Farm. *Energies* **2013**, *6*, 2605–2623.
8. Dawkins, M.S.; Donnelly, C.A.; Jones, T.A. Chicken welfare is influenced more by housing conditions than stocking density. *Nature* **2004**, *427*, 342–344.
9. Medio Millón de Pollos Mueren por el Fuerte Calor de los Últimos Días. Available online: http://elpais.com/diario/2003/06/17/cvalenciana/1055877480_850215.html (accessed on 12 May 2014).

10. Korea Heat Wave Kills Off 830,000 Chickens (in August 2012). Available online: http://www.worldpoultry.net/Broilers/Health/2012/8/S-Korean-heat-wave-kills-off-830000-chickens-WP010736W/ (accessed on 12 May 2014).
11. Blanes-Vidal, V.; Guijarro, E.; Balasch, S.; Torres, A.G. Application of computational fluid dynamics to the prediction of airflow in a mechanically ventilated commercial poultry building. *Biosyst. Eng.* **2008**, *100*, 105–116.
12. Mitchell, M.A.; Kettlewell, P.J. Physiological stress and welfare of broiler chickens in transit: Solutions not problems! *Poult. Sci.* **1998**, *91*, 1803–1814.
13. Sohail, M.U.; Hume, M.E.; Byrd, J.A.; Nisbet, D.J.; Ijaz, A.; Sohail, A.; Shabbir, M.Z.; Rehman, H. Effect of supplementation of prebiotic manan-oligosaccharides and probiotic mixture on growth performance of broilers subjected to chronic heat stress. *Poult. Sci.* **2012**, *91*, 2235–2240.
14. Department for Environment, Food and Rural Affairs(DEFRA). *Heat Stress in Poultry. Solving the Problem*; DEFRA: London, UK, 2008.
15. Norton, T.; Sun, D.; Grant, J.; Fallon, R.; Dodd, V. Applications of computational fluid dynamics (CFD) in the modeling and design of ventilation systems in the agricultural industry: A review. *Bioresour. Technol.* **2007**, *98*, 2386–2414.
16. Mistriotis, A.; de Jong, T.; Wagemans, M.J.M.; Bot, G.P.A. Computational fluid dynamics as a tool for the analysis of ventilation and indoor microclimate in agriculture buildings. *Neth. J. Agric. Sci.* **1997**, *45*, 81–96.
17. Bartzanas, T.; Kittas, C.; Sapounas, A.A.; Nikita-Martzopoulou, C. Analysis of airflow through experimental rural buildings: Sensitivity to turbulence models. *Biosyst. Eng.* **2007**, *97*, 229–239.
18. Harral, B.B.; Boon, C.R. Comparison of predicted and measured air flow patterns in a mechanically ventilated livestock buildings without animals. *J. Agric. Eng. Res.* **1997**, *66*, 221–228.
19. Pawar, S.R.; Cimbala, J.M.; Wheeler, E.F.; Lindberg, D.V. Analysis of poultry house ventilation using computational fluid dynamics. *Trans. ASABE* **2007**, *50*, 1373–1382.
20. Lee, I.B.; Sase, S.; Sung, S.H. Evaluation of CFD accuracy for the ventilation study of a naturally ventilated broiler house. *Jpn. Agric. Res. Q.* **2007**, *41*, 53–64.
21. Osorio, J.A.; Ferreira, I.F.; Oliveira, K.S.; Arêdes, M.; Oliveira, M. Modelling and experimental validation to estimate the energy balance for a poultry house with misting cooling. *Dyna* **2011**, *78*, 167–174.
22. Osorio, R.; Ferreira, I.F.; Osorio, J.A.; Oliveira, K.S.; Guerra, L.M. Modeling of the thermal environments in shed negative pressure tunnel cycle of chicks. *Rev. Fac. Nac. Agric.* **2013**, *66*, 7085–7093.
23. Mostafa, E.; Lee, I.B.; Song, S.H.; Kwon, K.S.; Seo, I.H.; Hong, S.W.; Hwang, H.S.; Bitog, J.P.; Han, H.T. Computational fluid dynamics simulation of air temperature distribution inside broiler building fitted with duct ventilation system. *Biosyst. Eng.* **2012**, *112*, 293–303.
24. Lacey, R.E.; Redwine, J.S.; Parnell, C.B. Particulate matter and ammonia emission factors for tunnel-ventilated broiler production houses in the Southern U.S. *Trans. ASAE* **2003**, *46*, 1203–1214.
25. Daghir, N.C. *Poultry Production in Hot Climates*; CAB International: Wallingford, UK, 2001.
26. Blanes-Vidal, V.; Guijarro, E.; Nadimi, E.S.; Torres, A.G. Development and field test of an on-line computerized instrumentation system for air velocity, temperature and differential pressure measurements in poultry houses. *Span. J. Agric. Res.* **2010**, *8*, 570–579.

27. Fluent Inc. *Fluent User's Guide*; Version 6.0; Fluent Inc.: Lebanon, NH, USA, 2001.
28. Patankar, S.V. *Numerical Heat Transfer and Fluid Flow*; Hemisphere Publishing Corporation: Washington, WA, USA, 1980.
29. Launder, B.E.; Spalding, D.B. The numerical computation of turbulent flows. *Comput. Method. Appl. Mech.* **1974**, *3*, 269–289.
30. Fluent Inc. *Gambit User's Guide*; Version 2.0; Fluent Inc.: Lebanon, NH, USA, 2001.
31. Bjerg, B.; Svidt, K.; Zhang, G.; Morsing, S.; Johnsen, J.O. Modeling of air inlets in CFD prediction of airflow in ventilated animal houses. *Comput. Electron. Agric.* **2002**, *34*, 223–235.
32. Calvet, S.; Cambra-López, M.; Blanes-Vidal, V.; Estellés, F.; Torres, A.G. Ventilation rates in mechanically ventilated commercial poultry buildings in Southern Europe: Measurement system development and uncertainty analysis. *Biosyst. Eng.* **2010**, *106*, 423–432.
33. American Society of Heating, Refrigerating and Air-Conditioning Engineers (ASHRAE). *ASHRAE Fundamentals Handbook*; American Society of Heating, Refrigerating and Air-Conditioning Engineers Inc.: Atlanta, GA, USA, 2001.
34. Testo Inc. Homepage. Available online: http://www.testo.com (accessed on 12 May 2014).
35. Heber, A.J.; Boon, C.R.; Peugh, M.W. Air patterns and turbulence in an experimental livestock building. *J. Agric. Eng. Res.* **1996**, *64*, 209–226.
36. Oberkampf, W.L.; Trucano, T.G. Verification and validation in computational fluid dynamics. *Progr. Aerosp. Sci.* **2002**, *38*, 209–272.
37. TFD. Omega Engineering, Inc. Available online: http://www.omega.com/Temperature/pdf/TFD_RTD.pdf (accessed on 12 May 2014).
38. Sensortechnics Inc. Available online: http://www.sensortechnics.com (accessed on 12 May 2014).
39. SAS Institute Inc. *SAS User's Guide: Statistics*; Version 6.12; SAS Institute Inc.: Cary, NC, USA, 1998.
40. Posner, J.D.; Buchanan, C.R.; Dunn-Rankin, D. Measurement and prediction of air flow in a model room. *Energ. Build.* **2003**, *35*, 515–526.
41. Lott, B.D.; Simmons, J.D.; May, J.D. Air velocity and high temperature effects on broiler performance. *Poult. Sci.* **1998**, *77*, 391–393.
42. Zuidhof, M.J.; Schneider, B.L.; Carney, V.L.; Korver, D.R.; Robinson, F.E. Growth, efficiency, and yield of commercial broilers from 1957, 1978, and 2005. *Poult. Sci.* **2014**, *93*, 2970–2982.